Electron- and Neutrino-Nucleus Cross Sections using Spectral Functions

Hiroki NAKAMURA
Department of Physics, Waseda University, Tokyo 169-8555, Japan
Ryoichi SEKI
Department of Physics and Astronomy, California State University, Northridge, Northridge, CA 91330, USA
W. K. Kellogg Radiation Laboratory, California Institute of Technology, Pasadena, CA 91125, USA
Makoto SAKUDA
Department of Physics, Okayama University, Okayama 700 -8530, Japan

Abstract

We examine various nuclear effects in the initial and final states of lepton scattering by calculating quasi-elastic and quasi-free $\Delta(1232)$ production cross sections. Comparison of the calculations with ^{16}O(e,e') data in the 700 – 1200 MeV incident energy shows that the use of the spectral function yields much more realistic cross sections than the Fermi gas model does. The application of our examination has a good promise in the application to neutrino scattering.

1. Introduction

As new and precise neutrino oscillation experiments are planned and some of them begin soon, reliable calculations of observables in neutrino-nucleus reactions will become vital. Our final goal is to meet this challenge to calculate them precise enough for the precision that will be reached by these experiments. By doing so, we expect that not only the calculation would be instrumental for the precise determination of the neutrino masses, but also they would reveal new interesting nuclear physics such as those associated with the axial currents in nuclei. In this contribution, we report the present status of our calculation on quasi-elastic scattering and on quasi-free $\Delta(1232)$ production, and update the results that we have reported in the previous neutrino workshops [1, 2].

We formulate neutrino-nucleus interactions as a sum of neutrino-nucleon interactions under the impulse approximation, under the assumption that the nuclear weak current is a sum of the nucleonic weak currents. At the initial stage of the interaction, the incident neutrino interacts with a nucleon in nucleus,

pp. 183–192

which carries the momentum and energy determined by nuclear structure. The energy-momentum spectrum of bound nucleons must be realistic for the energy-momentum transfer involved in the neutrino reactions under consideration. In the high-energy scattering of our interest, the magnitude of the transfer is mostly too large to be appropriately described by Fermi gas model or even by mean-field models such as simple shell models. The best candidates of the spectrum presently available are those provided by the spectral functions constructed from a many-body calculation using realistic nucleon-nucleon potentials. In this work, we use the spectral function obtained by Benhar *et al.* [3], and compare the cross sections that are calculated by it and by Fermi gas model, together with experimental electron scattering data.

After the initial interaction, the neutrino-nucleus reaction undergoes the final-state interactions that involve various nuclear effects. In our comparison, we also examine various models describing the final-state interactions.

2. Basic formalism

Our basic formalism is the same for the electron- and neutrino-nucleus interactions. The formalism for the quasi-elastic and also quasi-free Delta production cross sections has been described in the previous neutrino workshops [1, 2]. Here, we include only the key expressions relevant to the present discussions.

Quasi-elastic cross section is written as

$$\frac{d\sigma}{dE'd\Omega} = \frac{k'}{8(2\pi)^4 M_A E} \int d^3\boldsymbol{p} F(\boldsymbol{p},\boldsymbol{q},\omega) \sum_{\rm spin} |\mathcal{M}_{\ell N}|^2, \tag{1}$$

where E is the incident lepton energy, M_A the target nucleus mass, and E' and k' are the energy and momentum of the scattered lepton, respectively. $\mathcal{M}_{\ell N}$ is the invariant amplitude of lepton-nucleon elastic scattering. $F(\boldsymbol{p},\boldsymbol{q},\omega)$ is proportional to the imaginary part of the $1p1h$ Green's function, expressed in terms of the momentum and energy transferred to the nucleus, $\boldsymbol{q}$ and ω, respectively, and also of the nucleon momentum bound in the nucleus, $\boldsymbol{p}$. For high-energy reactions, $F(\boldsymbol{p},\boldsymbol{q},\omega)$ is approximately factorized as

$$F(\boldsymbol{p},\boldsymbol{q},\omega) = \frac{M_A}{(2\pi)^2 V} \int d\omega' P_h(\boldsymbol{p},\omega') P_p(\boldsymbol{p}+\boldsymbol{q},\omega-\omega'), \tag{2}$$

where $P_h(\boldsymbol{p},\omega)$ and $P_p(\boldsymbol{p},\omega)$ are the $1h$ and $1p$ Green's functions, respectively. V is the normalization volume. Apart from a simple kinematical factor as shown in Eq. (4) below, $P_h(\boldsymbol{p},\omega)$ is referred as the spectral function and describes the probability to remove a nucleon of the momentum $\boldsymbol{p}$ with the removal energy ω.

$P_p(\boldsymbol{p},\omega)$ describes the final-state interactions of the knocked-out nucleon. Thus, as they are combined, $P_h(\boldsymbol{p},\omega)$ and $P_p(\boldsymbol{p},\omega)$ fully describe dynamics of the response of the nucleon involved in the lepton scattering.

The form factors that we use in the invariant amplitudes of electron-nucleon scattering are of non-dipole forms, taken from Ref. [4, 5]. The axial form factor used in the invariant amplitude of neutrino-nucleon scattering is of the dipole form with $M_A = 1.07$ GeV.

Quasi-free Δ resonance production cross sections are calculated also from Eq. (1) by using the invariant amplitude of the Δ production [6]. The N-Δ transition form factors are taken from a recent work of Ref. [7].

3. Nuclear Effects

As noted above, nuclear effects are included in $P_h(\boldsymbol{p},\omega)$ and $P_p(\boldsymbol{p},\omega)$. In the following, we discuss $P_h(\boldsymbol{p},\omega)$ and $P_p(\boldsymbol{p},\omega)$ separately.

3.1. $P_h(\boldsymbol{p},\omega)$: the initial nuclear state

3.1.1. a. Fermi Gas Model

In our formalism, Fermi gas model, widely used in Monte Carlo simulation, corresponds to:

$$P_h(\boldsymbol{p},\omega) = \frac{V}{E_p}\theta(P_F - p)\delta(E_p + \omega)\ , \tag{3}$$

where $E_p = \sqrt{p^2 + M^2} - E_B$ is the initial nucleon energy with the effective binding energy E_B and with $|\boldsymbol{p}| = p$. The Fermi Gas model used here is a relativistic one as formulated some years ago [8, 9]. Equation (3) shows that the nucleons are assumed to be non-interacting, experiencing E_B at the zero temperature.

For numerical calculations for oxygen, we take P_F to be 225 MeV and E_B to 27 MeV [10].

3.1.2. b. Spectral Function

The spectral function that we use has been obtained from a many-body calculation with correlated nuclear-state basis together with a realistic nucleon-nucleon interaction, combined with shell model and local density approximation [3]. As such, the spectral function is quite realistic and includes all physics relevant to the high-energy lepton-nucleus scattering, especially realistic short-range nuclear correlations important to large momentum transfers.

$P_h(\boldsymbol{p},\omega)$ is directly related to the spectral function $P(\boldsymbol{p},\omega)$ as

$$P_h(\boldsymbol{p},\omega) = \frac{1}{E_p}P(\boldsymbol{p},\omega)\ . \tag{4}$$

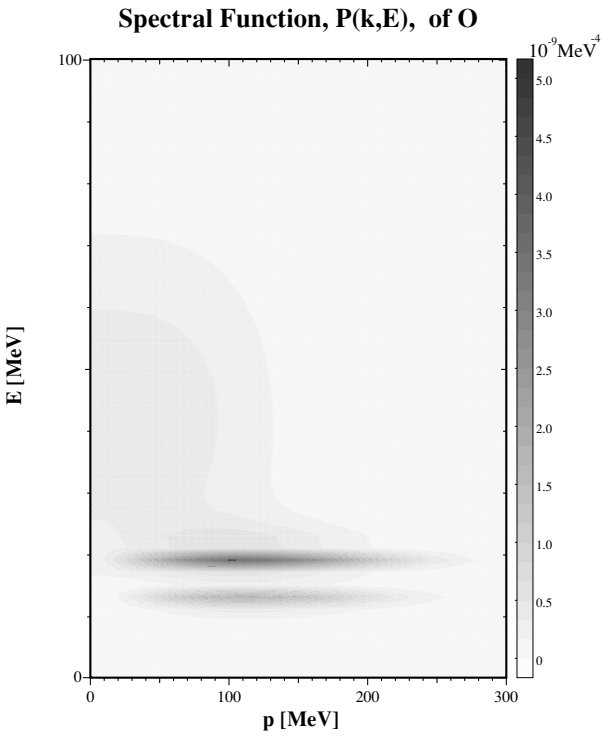

Fig 1. Density plot of spectral function $P(\boldsymbol{p}, E)$ of ^{16}O [3].

In Fig. 1, we illustrate $P(\boldsymbol{p}, \omega)$ that have been obtained by O. Benhar et al. [3] and are used for our oxygen calculations.

3.2. $P_p(\boldsymbol{p}, \omega)$: final-state Interactions

We examine various models of $P_p(\boldsymbol{p}, \omega)$ that describes the final-state interactions of the knocked-out nucleon with the other nucleons in the nucleus. The models are:

a. Fermi gas model that includes the simple version of Pauli blocking effects in the standard form,

and the three models that we use with the spectral function,

b. Plain wave impulse approximation,

c. Modified Pauli blocking, and

d. Optical potential model.

The first three models, a. – c. are expressed as

$$P_p(\boldsymbol{p}', \omega) = \frac{V}{E'_p} n_p(p') \delta(E'_p - \omega) \ , \tag{5}$$

where $E'_p = \sqrt{p'^2 + M^2}$ and $p' = |\boldsymbol{p}'|$ are the final-state energy and (the magnitude of) momentum of the (knocked-out) nucleon. Here, we neglect the nuclear binding energy. $n_p(p')$ is the momentum distribution of the nucleon in the final state, and takes different forms in different models as described below.

3.2.1. a. Fermi Gas Model: simple Pauli blocking

In the Fermi gas model, $n_p(p')$ is written as

$$n_p(p') = \theta(p' - P_F) \ . \tag{6}$$

Through $\theta(p' - P_F)$, $P_p(\boldsymbol{p}, \omega)$ describes Pauli blocking, the knocked-out nucleon momentum being blocked off when it is less than the Fermi momentum P_F.

3.2.2. b. Plain Wave Impulse Approximation

The plain-wave impulse approximation simply ignores the final state interactions. That is, we simply set

$$n_p(p') = 1 \ . \tag{7}$$

3.2.3. c. Modified Pauli Blocking

Here, we apply a more realistic version of Pauli blocking effect through the use of the nucleon momentum distribution that satisfies a sum rule of $P_h(\boldsymbol{p}, \omega)$ and $P_p(\boldsymbol{p}, \omega)$ [12]:

$$\int (P_h(\boldsymbol{p}, \omega) + P_p(\boldsymbol{p}, \omega)) \omega d\omega = V \ , \tag{8}$$

where $V = 1/[(2\pi)^3 \rho]$ for the uniform nuclear matter of the density ρ. Note that the weighted integration $\int \omega d\omega$ instead of the standard $\int d\omega$ in the literature comes from our definition of $P_h(\boldsymbol{p}, \omega)$ and $P_p(\boldsymbol{p}, \omega)$ as introduced in Eq. (2). Because the initial and final momentum density distributions, $n_h(p)$ and $n_p(p)$, respectively, are related to $P_h(\boldsymbol{p}, \omega)$ and $P_p(\boldsymbol{p}, \omega)$ as

$$\begin{aligned} n_h(p) &= \frac{1}{V} \int P_h(\boldsymbol{p}, \omega) \omega d\omega \\ n_p(p) &= \frac{1}{V} \int P_p(\boldsymbol{p}, \omega) \omega d\omega \ , \end{aligned} \tag{9}$$

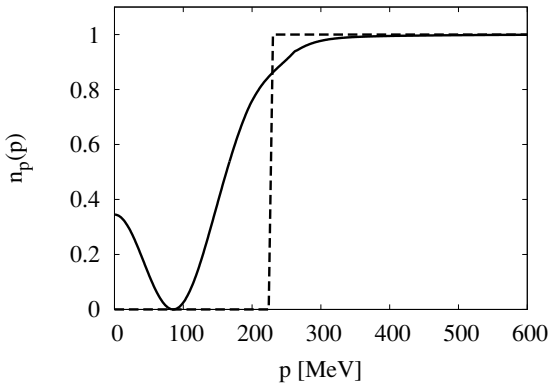

Fig 2. $n_p(p)$ for Modified Pauli blocking (solid line), as a function of the momentum, p, compared with $n_p(p)$ of the step function form for Fermi gas (dashed line).

we have

$$n_p(p) = 1 - (2\pi)^3 \rho \int P_h(\boldsymbol{p}, \omega) d\omega \ . \tag{10}$$

ρ is taken to be the average density where the neutrino reaction takes place, and is set to be $0.4\rho_0$ in terms of the nuclear matter density $\rho_0 = 0.16$ fm^{-3}. For this choice, $n_p(p)$ remains non-negative. Figure 2 shows $n_p(p)$ thus constructed in comparison to the Fermi gas $n_p(p)$. The small $n_p(p)$ distribution for $p < 100$ MeV/c appears because the two plateaus in $P(\boldsymbol{p}, E)$ with the two nearly constant values of E do not reach $p = 0$ but spread out and diminish with tails, as shown in Fig. 1. It is a consequence of the realistic momentum distribution $n_p(p)$ in finite nuclei.

3.2.4. d. Optical Potential Model

In this model, the final-state interactions of the knocked-out nucleon are described with its reactions with the other nucleons in the nucleus as it goes out, through the nucleon-nucleus optical potential. The model can be complicated, but its simple version yields [13]

$$P_p(\boldsymbol{p}', \omega) = \frac{V}{E'_p} \frac{W(\boldsymbol{p}')/\pi}{(\omega - E'_p)^2 + W^2(\boldsymbol{p}')/4} \ , \tag{11}$$

where $W(\boldsymbol{p}')$ is the imaginary part of the nucleon-nucleus potential, depending on the momentum (and generally also on the energy) of the knocked-out nucleon. Here, we take it to be

$$W(\boldsymbol{p}') = \frac{1}{2} v(\boldsymbol{p}') \rho \sigma_{NN}(\boldsymbol{p}') \tag{12}$$

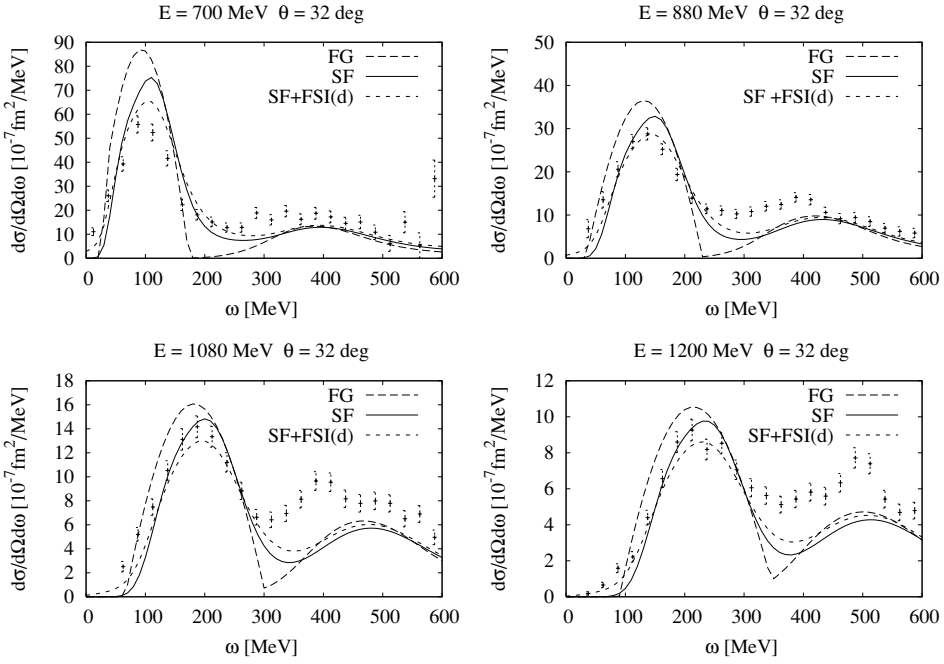

Fig 3. Combined cross sections of electron-^{16}O quasi-elastic scattering and quasi-free Δ resonance production. FG (shown in dash curves) is the use of Fermi gas model; SF (shown in solid curves) is the use of the spectral function with no final-state interaction (i.e. in plain wave impulse approximation); and SF+FSI(d) (shown in dot curves) is the use of the spectral function with the final state interaction of optical potential. The (e, e') experimental data [11] are shown for comparison.

in the lowest-order approximation of the optical potential. Here, $v(\boldsymbol{p}')$ is the velocity of the knocked-out nucleon with the momentum $\boldsymbol{p}'$. As a simple evaluation, we set the nucleon density, ρ, to be that of the nuclear matter, ρ_0, and the nucleon-nucleon cross section, σ_{NN}, to be 40 mb. ρ depends on the location in the nucleus, where the neutrino reaction takes place. The values of these quantities, which are used in the simple expression of W Eq. (12), should be the effective ones averaged over the relevant variables. W that we use here as a simple evaluation is thus an overestimate in some degree.

4. Numerical results

4.1. Electron scattering

In Fig. 3 we compare the electron-^{16}O scattering cross sections calculated in various ways, together with experimental data. The comparison is made for the kinematical set where the experimental data are available: the scattering angle

$\theta = 32°$, and the incident energy $E = 0.7$, 0.88, 1.08 and 1.2 GeV [11]. The calculated cross sections are shown for the use of the Fermi gas model and of the spectral function with no final state interaction (that is, in the plain wave impulse approximation) and with the final state interaction of the optical potential form.

Each curve of the calculated cross section in the figure is a sum of the quasi-elastic and quasi-free Δ production cross sections. Each curve thus consists of two bumps, that of the quasi-elastic scattering at the low energy side and that of the quasi-free Δ production at high energy side, with the two contributions overlapping between the two bumps.

The figure shows that for the quasi-elastic cross sections, the spectral function gives a better agreement with the data even without the final state interaction (shown as SF), than Fermi gas model (shown as FG). The Fermi gas model much overestimates at all energies. When the final state interaction is include in the spectral function calculation (as the optical potential, shown as SF+FSI), the agreement with data improves for the incident energy below 1 GeV, but the agreement does not necessarily improve above 1 GeV. The optical potential parameters used seem to be indeed an overestimate, but such a simple parameterization is clearly inadequate to describe the energy-dependent behavior and requires a further refinement.

At all energies, the quasi-elastic cross sections by the use of the spectral functions with (SF+FSI) and without (SF) the final state interaction have tails at higher energy transfers, while the Fermi gas cross section (FG) does not. The appearance of the tails is a consequence of the large momentum components in the nucleon momentum distribution, which is generated by the short-range correlations.

At the energy region higher than the quasi-elastic scattering, all calculated cross sections are below the data. In our calculation, we have included the contribution from the quasi-free Δ production but *not the contributions from the non-resonant pion production*, which are known to be appreciable. Inclusion of these contributions is our future study, together with the final state interactions of the pions produced.

4.2. Neutrino scattering

We have applied the various forms of nuclear effects also to neutrino scattering under different kinematical conditions. Here, we focus on the momentum-transfer dependence of the neutrino cross section, especially at the small momentum-transfer region near the forward direction. The region is of current interest because the coherent scattering contribution experimentally determined appears to be much less than the expected in this region, as reported in this workshop [14].

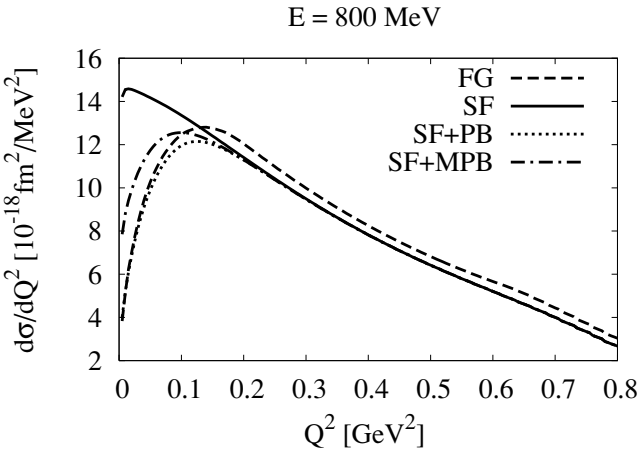

Fig 4. $^{16}\mathrm{O}(\nu_\mu, \mu^-)$ quasi-elastic cross section as a function of square of the momentum transfer Q^2 for the neutrino incident energy $E = 0.8$ GeV. The Fermi gas model is shown as a dash curve (FG), and three different versions of the spectral function model are shown as: with no final state interaction as a solid curve (SF), with the final state interaction of the simple Pauli blocking (the same as that in the Fermi gas model) as a dot curve (SF+PB), and with the final state interaction of the modified Pauli blocking as a dot-dash curve (SF+MPB).

In Fig. 4, we show $^{16}\mathrm{O}(\nu_\mu, \mu^-)$ quasi-elastic cross section calculated in various ways, as a function of the four-momentum square, Q^2. In the figure, we also include the cross sections for the spectral function model combined with $n_p(p')$ of the simple Pauli blocking Fermi gas model (shown as SF+PB) and with $n_p(p')$ of the modified Pauli blocking (shown as SF+MPB).

At small Q^2, the figure shows that the spectral function model without the final state interaction (SF) fails to show a depression in the small Q^2 region, while all other models do show it. All other models include the Pauli blocking effects in the final state interaction, and the Pauli blocking effects are thus responsible for the reduction of the cross section near the forward direction. The simple Pauli blocking of the step function form Eq. (6) provides a stronger depression (as seen in FG and SF+PB) than the modified Pauli blocking (SF+MPB).

Figure 4 illustrates the importance of the realistic evaluation of the Pauli blocking effect in the final state interactions and also the usefulness of our approach in the neutrino-nucleus scattering. The calculation can be tested by the electron scattering data taken recently with Carbon target at 1.2 GeV [15].

5. Conclusions

We have calculated electron-nucleus cross sections over the incident energy range of 700 – 1200 MeV by using various forms of nuclear effects in the initial and final states of the neutrino interaction in the nucleus. Comparison of the calculated cross sections with the experimental data shows that the use of the spectral function yields much more realistic cross sections than the Fermi gas model does, the latter failing to describe some of important features. The application of our examination is expected to have a good promise in the application to neutrino scattering.

Acknowledgments

We thank O. Benhar for providing us his ^{16}O spectral function. This work is supported by the U. S. Department of Energy under grant DE-FG03-87ER40347 at CSUN and by the U. S. National Science Foundation under grant 0244899 at Caltech.

References

[1] H. Nakamura and R. Seki, Nucl. Phys. Proc. Suppl. **112** (2002) 197.
[2] H. Nakamura, R. Seki and M. Sakuda, Nucl. Phys. Proc. Suppl. **139** (2005) 201.
[3] Private communication from O. Benhar. The method of the calculation is described in: O. Benhar, A. Fabrocini, S. Fantoni, and I. Sick, Nucl. Phys. **A579** (1994) 493; and references therein.
[4] E. J. Brash, A. Kozlov, S. Li and G. M. Huber, Phys. Rev. C **65** (2002) 051001.
[5] P. E. Bosted, Phys. Rev. C **51** (1995) 409.
[6] C.H. Llewellyn Smith, Phys. Rept. **3** (1972) 261.
[7] E. A. Paschos, J. Y. Yu and M. Sakuda, Phys. Rev. D **69** (2004) 014013.
[8] R.A. Smith and E.J. Moniz, Nucl. Phys. B **43** (1972) 605.
[9] E. J. Moniz, Phys. Rev. **184** (1969) 1154.
[10] E.J. Moniz, I. Sick, R.R. Whitney, J.R. Ficenec, R.D. Kephart and W.P. Trower, Phys. Rev. Lett. **26** (1971) 445.
[11] M. Anghinolfi *et al.*, Nucl. Phys. A **602** (1996) 405.
[12] O. Benhar, A. Fabrocini, and S. Fantoni, Nucl. Phys. A **550** (1992) 201.
[13] O. Benhar, A. Fabrocini, S. Fantoni, G. A. Miller, V. R. Pandharipande and I. Sick, Phys. Rev. C **44** (1991) 2328.
[14] M. Hasegawa, in this proceedings.
[15] JLAB E04-001 experiment (JUPITER).